

An Automatic High-Speed Rail CPIII Detection System With Multi-Sensor Fusion

Yi Han^{*}, Yunde Zhao, Saiwei Zhang and Dongsheng Zhang

School of Automobile, Chang'an University, Xi'an, Shaanxi, 710064, China

Abstract: In order to measure the CPIII control network of high-speed rail quickly and accurately, we propose an automatic high-speed rail CPIII detection system with multi-sensor fusion. The system is based on binocular stereo vision. Dual array camera, Matrox Solios XCL frame grabbers and IPC are used to build the CPIII image acquisition environment. The photoelectric encoder is the trigger of camera. The software HALCON is used to recognize the CPIII image and get the pixel coordinates of CPIII markers' center. Then, we use the intersection measurement principle to calculate the central position of CPIII markers in camera coordinate system. The function of CPIII image acquisition, automatic identification, calculation are integrated by Visual Studio 2008. Finally, we can realize the non-contact dynamic test of CPIII. The CPIII automatic detection system can also be combined with the IMU, GPS, gauge sensors and other detection tools into a small track inspection vehicle and realized the real-time measurement of orbital parameters.

Keywords: Automatic identification, calibration, CPIII, High-speed rail, halcon, positioning.

1. INTRODUCTION

High-speed railway track condition is an important factor related to the safety operation of the train. Therefore the accurate measurement of rail is necessary whether in construction stage or in maintenance stage [1, 2]. The traditional measurement method is to use the total station, rail gauge and other tools for manual inspection. With the rapid development of sensor technology and computer technology, many developed countries have started using the two-dimensional photoelectric sensors (such as CCD, PSD, CMOS sensor). The original detection technology have been replaced by the detection techniques based on laser and camera [3]. The new method has greatly improved the speed, precision, reliability and stability of detection system. So the detection techniques based on laser and camera have become the mainstream of the track detection systems in various countries, such as Japan, the United States, Austria, Germany, Italy, France.

The East-i Comprehensive Test Train [4] made by Japan can detect the track geometry parameters, the catenary, communication signals, the wheel-rail forces, environmental noise and other projects, the maximum test speed is 275km/h [5]. Laserail track measurement system [6, 7] made by US ImageMap company use a laser imaging and high-speed image processing technology to replace the photoelectric servo technology [8], the maximum test speed is 300km/h. The maximum test speed of EM-250 inspection vehicle made by Plasser Company can reach 250km/h, this type of track inspection vehicle adopts the inertial reference measurement

technology, photovoltaic conversion technology and multi-processing technology. It not only can measure the orbital geometry and vehicle vibration parameters, but also can get the parameters of the rail, the wheel-rail forces and record environmental image. The OMWE and RAILAB inspection vehicle made by Germany in the 1980s and 1990s respectively can detect the rail with the speed of 300km/h. The characteristics of its technical is the using of inertial measurement platform [9] constructed by three gyro accelerometers and three servos to detect the orbital geometry parameters. The platform can combined with photoelectric sensors, computer vision [10-15] to get the height, horizontal, alignment of the orbital. Italian Archimedes detection vehicle equipped with lasers, sensors (such as photoelectric sensors, speed sensors, temperature sensors) and IMU. The function mainly includes the detection of track geometry, rail sections, rail wear, current performance between catenary and Pantograph-Catenary, communication signals, body, axle box acceleration, wheel-rail forces. Each subsystem of Archimedes comprehensive test train [11] has a separate database for storing data and the various subsystems can keep pace in speed, time and space. In order to guide the track maintenance scientifically, the test data of all subsystems from the central database were aggregated from the central database and transmitted over a wireless network to the RFI (data processing center) for comprehensive analysis and comparison. The MGV comprehensive inspection vehicle which is made by French can reach the speed of 320 km/h. The detection projects of the vehicle mainly includes current performance between catenary and Pantograph-Catenary, communication signals, track geometry, rail sections and surfaces, line environment, fasteners, sleepers, ballasts and so on. The GJ-6 orbital inspection vehicle made by China represents the newest technology in domestic track detection. GJ-6 track detection system uses high-speed image processing [12], photoe-

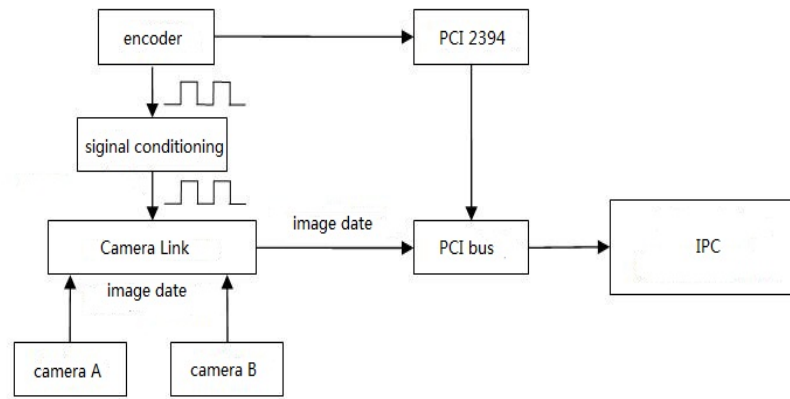


Fig. (1). Hardware structure.

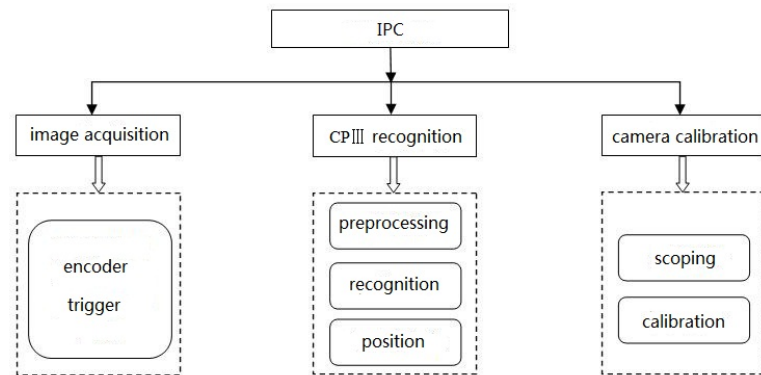


Fig. (2). Software structure.

lectric measurements, the gyro platform, digital filtering, mileage positioning, high-speed computer data processing in real-time and other advanced technology. The characteristics are high-speed, accurate, reliable and stable [13].

At present, the total station, rail gauge and other tools are commonly used in domestic railway track inspection during the construction. The method is easily influenced by the external environment and the detection efficiency is low [14]. In the operation and maintenance stage, track inspection trains are used for the test of rail. Even though the inspection trains have the advantage of high detection speed and high precision, it is dependent on the catenary. What's more, it has complex organizations and high cost. During the CP III retest stage, it can not be used. To solve these problems, we design a high-speed rail CP III automatic detection system with multi-sensor fusion. The system is based on binocular stereo vision. It also can be combined with the IMU, GPS, gauge sensors and other detection tools to realize the detection of gauge, alignment, height and horizontal. This will not only meet the demand of the CP III control network retest and improve the precision, but also have the advantage of simple structure, easy to detect and small Catenary-dependent.

2. MEASURING PRINCIPLE AND SYSTEM CONFIGURATION

This system is based on the principle of binocular stereo vision technology, according to the feature of non-contact

measurement technology: high-precision, high efficiency and

low cost, a high-speed rail CP III automatic detection system of multi-sensor fusion is studied and developed. The system is mainly to establish a CP III control network testing as the main platform for the detection of high-speed railway routine maintenance, providing a convenient, reliable, and accurate way to measure CP III control network. At the same time, the system which is based on the platform can measure the gauge, rail-to, the level of inequality argument by combining with inertial components, and other measurement tools.

The hardware part of the system is mainly consisted of two linear array camera, IPC, Camera Link frame grabber interface, optical encoder, etc. The Fig. (1) has shown the hardware configuration. Photoelectric encoder generates a pulsed square wave signal with the rotation of the wheels. The signal gets the stable A, B phase pulse after filtering and signal amplification. Then, the pulse is transmitted into the Camera Link frame grabber to control the shoot of camera. When the Camera Link frame grabber receives a rising edge of the square wave pulse, line scan cameras scan one line. In order to achieve an image mileage positioning function, we give the count value of PCI 2394 card to the frame image at the moment.

The software part of system which is based on MFC is developed on Visual Studio 2008 platform to design and develop CP III automatic detection software. The software mainly includes image acquisition module, CP III recognition

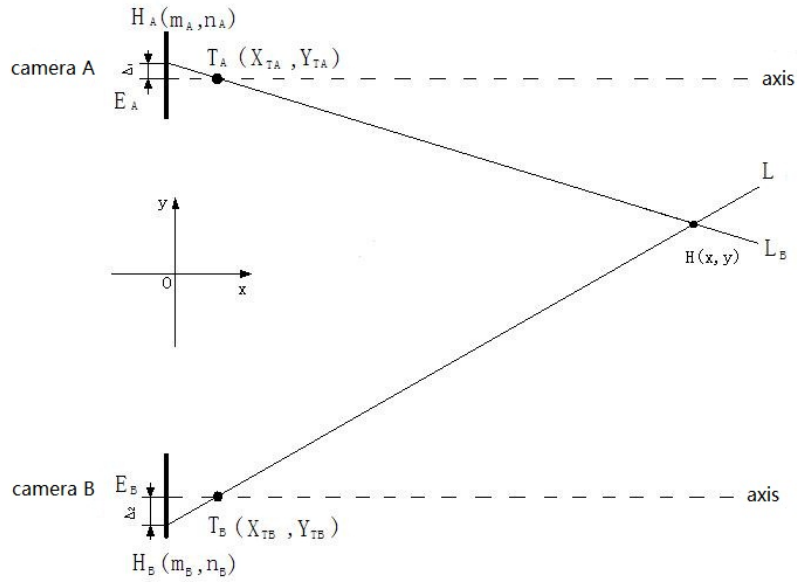


Fig. (3). Binocular stereo vision system.

module and camera calibration module. The Fig. (2) has shown the software structure.

3. SYSTEM CALIBRATION

Camera calibration is a very important step in the transition from 2D images transform into 3D computer vision [16]. In this measurement system, calibration is for the purpose of getting the corresponding relationship between input variables and output variables in CPⅢ automatic measurement system. The Fig. (3) has shown the structure of the binocular stereoscopic measurement system, the origin of the camera coordinate system is O, the input variable is the imaging position of CPⅢ markers' center H (x, y) in linear array camera A and B respectively during the calibration, the system constant is the center position of optical, the focal length and inclination, etc , the output variable is CPⅢ markers' center position coordinate in the camera coordinate system.

The imaging position of CPⅢ markers' center H (x, y) on two linear array CCD is the intersection of LA with linear CCD A H_A (m_A, n_A) and L_B with linear array CCD B H_B (m_B, n_B). The points relative to the image imaging center (optical axis imaging position, linear array image center) E_A, E_B's deviations are Δ₁ and Δ₂. Owing to the deviation of the center of the imaging position CPⅢ marker line on the CCD array with respect to the optical axis of the imaging position is proportional to the deviation of the coordinates of the pixel position in the acquisition image with respect to the image center, the center marker located CPⅢ two line pixels in the camera image coordinates are a₁, a₂, the deviations is (2048-a₁), and (2048-a₂). Set the slope of linear L_A and L_B as k_A, k_B, using slope-intercept form linear formula:

$$y = k_i x + b_i (i = A, B) \tag{1}$$

k_A and k_B in the slope-intercept form equation can be calculated from the coordinate values of H_A, T_A, H_B, T_B in the camera coordinate system:

$$k_A = \frac{n_A - y_{TA}}{m_A - x_{TA}} \tag{2}$$

$$k_B = \frac{n_B - y_{TB}}{m_B - x_{TB}} \tag{3}$$

We can get the value of b_A and b_B by formula (1):

$$b_A = y_{TA} - k_A x_{TA} \tag{4}$$

$$b_B = y_{TB} - k_B x_{TB} \tag{5}$$

In practice, the denominator of formula (2), (3) are not zero and k_A ≠ k_B. CPⅢ marker's center H (x, y) is the intersection of L_A and L_B, so, the position of H (x, y) in the camera coordinate system is:

$$x = \frac{b_B - b_A}{k_A - k_B} = \frac{(k_A x_{TA} - k_B x_{TB}) - (y_{TA} - y_{TB})}{k_A - k_B} \tag{6}$$

$$y = \frac{k_A b_B - k_B b_A}{k_A - k_B} = \frac{k_A k_B (x_{TA} - x_{TB}) - (k_B x_{TA} - k_A x_{TB})}{k_A - k_B} \tag{7}$$

Put k_A, k_B, b_A, b_B into formula (4) and (5). We can get the formula (8) and (9).

$$x = f_x(m_A, n_A, m_B, n_B, x_{TA}, y_{TA}, x_{TB}, y_{TB}) \tag{8}$$

$$y = f_y(m_A, n_A, m_B, n_B, x_{TA}, y_{TA}, x_{TB}, y_{TB}) \tag{9}$$

In the formula, x and y are the function of m_A, n_A, m_B, n_B, x_{TA}, y_{TA}, x_{TB}, y_{TB}, focal length, inclination, optical center coordinates are fixed with the process of capturing image every time, only the parameters m_A, n_A, m_B, n_B are changing with the motion of the input variables H (x, y). So the two formulas above can be written as the following form.

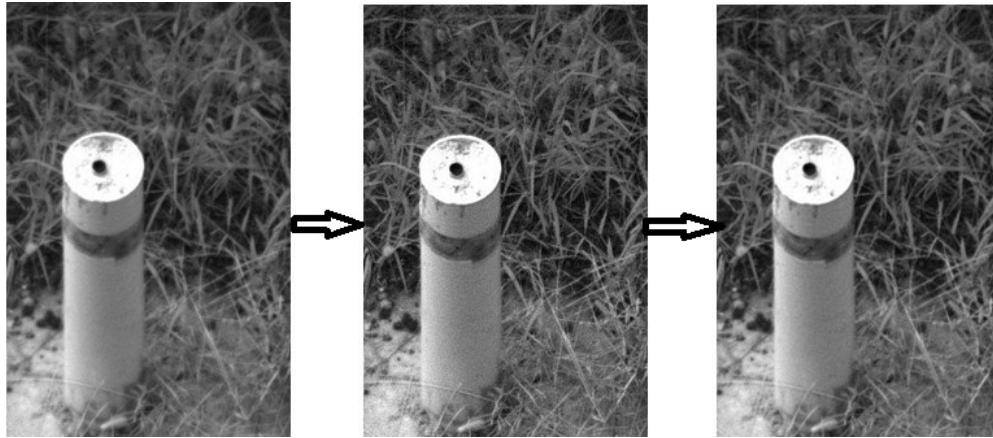


Fig. (4). Image pre-processing.

$$x = \frac{c_0(2048 - a_1)(2048 - a_2) + c_1(2048 - a_1) + c_2(2048 - a_2) + c_3}{c_4(2048 - a_1)(2048 - a_2) + c_5(2048 - a_1) + c_6(2048 - a_2) + c_7} + c_8 \quad (10)$$

$$y = \frac{c_9(2048 - a_1)(2048 - a_2) + c_{10}(2048 - a_1) + c_{11}(2048 - a_2) + c_{12}}{c_{13}(2048 - a_1)(2048 - a_2) + c_{14}(2048 - a_1) + c_{15}(2048 - a_2) + c_{16}} + c_{17} \quad (11)$$

In the formula above, $c_i (i = 0, 1, \dots, 17)$ is the polynomial coefficients based on the variable $(2048 - a_1)$ and $(2048 - a_2)$. Owing to the parameters of the ranging system, such as focal length, inclination, optical center coordinates are constant during image acquisition, so the system is a constant system, the correspondence between the input variables and output variables keep unchanged. We don't need to solve or get each constant parameter during the measurement, we just need to collect the calibration images at different distances and record the location parameters of calibration images in the camera calibration coordinates, using Marquardt method and general anti-global optimization method can calculate the value of the polynomial coefficients in formula (10) (11).

4. CPⅢ AUTOMATIC IDENTIFICATION

CPⅢ automatic identification include three parts: image preprocessing, image recognition and locating of the markers' central.

The main purpose of preprocessing image is to remove the interference information in the image and reduce the impact of recognition results by the interference information [17]. Firstly, we chose the operator emphasize to enhance image contrast, the calculate formula is (12). In the formula $T(r_k)$ represent the k -th gray level conversion function of original image. $\sum n_j / N$ represent the sum of gray levels of the pixels from 0 to j . N_j represents the the sum of the total number of pixels. $\sum P_r(r_k)$ represents the sum of the probability of the gray level occurrence from 0 to k . Then use gauss_image Gaussian blur the image to reduce image noise and reduce the level of detail, highlighting the outline feature, laying the groundwork for subsequent identification, which is calculated as formula (12). Pre-processing the image is shown in Fig. (4).

$$S = T(r_k) = \sum_{j=0}^k n_j / N = \sum_{j=0}^k P_r(r_k) \quad (12)$$

$$H(x, y) = \frac{1}{2\pi\sigma^2} e^{-\frac{x^2+y^2}{2\sigma^2}} \quad (13)$$

Image recognition, we find the object in the image based on the shape of the template matching. The algorithm can find the position of template in the picture, even if a part of the picture is occluded or interfered. It also is can not be influenced by the change of non-linear illumination [18]. In order to define the similarity of template matching, we define the first template of the target as a set of points $p_i = (r_i, c_i)^T$, the direction vector associated with each point is $d_i = (t_i, u_i)^T$, $i = 1, \dots, n$. Then use the target to create a template and calculate a direction vector $e_{r,c} = (v_{r,c}, w_{r,c})^T$ for each point (r, c) in the image. We can get the linear transformation model by $p'_i = A p_i$ and the corresponding direction vector $d'_i = (A^{-1})^T d_i$ obtained in the image. Calculate the direction vector and the sum the direction vector's dot product at the corresponding point of picture. Then take it as a post-match score and it is the conversion template similarity measurement at point q , the formula is as follows:

$$s = \frac{1}{n} \sum_{i=1}^n \frac{d_i^T e_{q+p'}}{\|d'_i\| \|e_{q+p'}\|} = \frac{1}{n} \sum_{i=1}^n \frac{t'_i v_{r+r'_i, c+c'_i} + u'_i w_{r+r'_i, c+c'_i}}{\sqrt{t_i'^2 + u_i'^2} \sqrt{v_{r+r'_i, c+c'_i}^2 + w_{r+r'_i, c+c'_i}^2}} \quad (14)$$

In order to realize the accuracy of the feature points in the image reach to sub-pixel, find the template points' closest point in the image through algorithm, so that the distances' sum of squares between these points and the corresponding line segment is minimum. The corresponding line segment of image point is defined by the tangent point and the tangent line of points in corresponding template. So the formula of the line, which is through the template points and tangent to the boundary of object is formula (15).

$$t_i(r - r_i) + u_i(c - c_i) = 0 \quad (15)$$

Use $q_i = (r'_i, c'_i)$ to represent the points in the image corresponding with the template point p_i . We can get the formula (16).

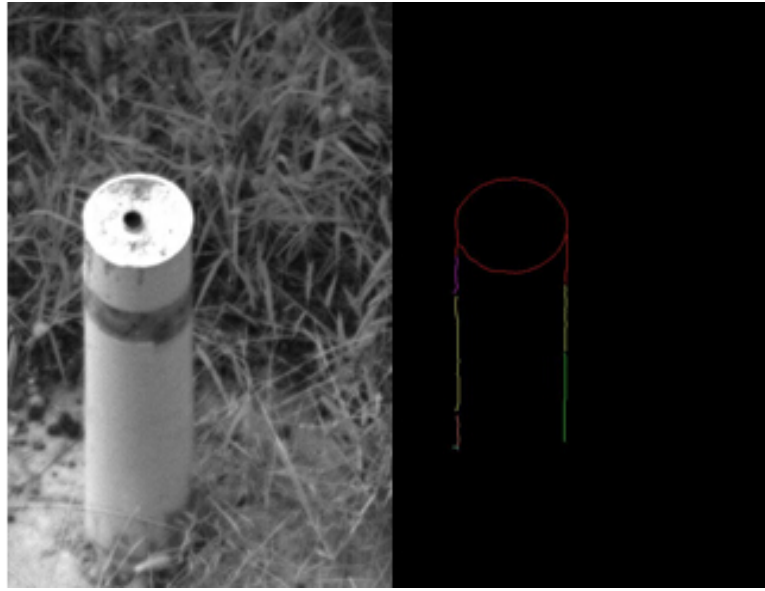


Fig. (5). Image recognition.

$$d(a) = \sum_{i=1}^n [t_i(r'_i(a) - r_i) + u_i(c'_i(a) - c_i)]^2 \rightarrow \min \quad (16)$$

If we obtain more accurate position and orientation parameters, the correspondence may be effected. So we can get higher accuracy by iterative optimization of pose parameters and correspondence. In HALCON, use operator create_shape_model and find_shape_model to generate templates and matching template respectively, the effect shown in Fig. (5).

The location of markers' center, extract the higher brightness oval area in template, use operator threshold to split images and find the light areas of CPIII. If the CPIII is not within the selected range, we can use the operator shape_trans to exchange all the border in the previous step and pixels inside the boundary region into new domain. Use operator reduce_domain to remove all parts beyond the threshold. Then extract the lighter areas contains CPIII and use the operator threshold again to obtained black areas of CPIII. According to the circular structure, use operator gen_contour_region_xld to create XLD contours and use operator fit_circle_contour_xld to fit the XLD circular outline, set circle formula as formula (17):

$$(x_i - x_0)^2 + (y_i - y_0)^2 = R^2 \quad (17)$$

In the formula (x_0, y_0) is the center, R is the radius, (x_i, y_i) is the edge point, $i = 1, \dots, N$, N is the number of edge points. Define the error as formula (18).

$$S = \sum_{i=1}^N [R^2 - (x_i - x_0)^2 - (y_i - y_0)^2]^2 \quad (18)$$

The coordinates of center (x_0, y_0) and radius R can be get by least square method. Finally, use operator gen_circle_contour_xld to get the pixel position a_1, a_2 , the

two positions are CPIII marker's center in the images get by camera A and B. The positioning process of marker's center has shown in Fig. (6).

Part of the code is as follows:

```
threshold (ImageGauss, Regions, 235, 255)
shape_trans (Regions, RegionTrans, 'convex')
reduce_domain (ImageGauss, RegionTrans, ImageReduced)
threshold (ImageReduced, Region, 0, 90)
gen_contour_region_xld (Region, Contours, 'border')
fit_circle_contour_xld (Contours, 'algebraic', -1, 0, 0, 3, 2, Row, Column, Radius, StartPhi, EndPhi, PointOrder)
gen_circle_contour_xld (ContCircle, Row, Column, Radius, 0, 6.28318, 'positive', 1)
```

5. THE CALCULATION OF CPIII MARKER'S CENTER

According to the calibration principle above, we collect the calibration images in different distances and record the location parameters of calibration images in camera coordinate system. Then, use the Marquardt method and general anti-global optimization method to calculate the values of the polynomial coefficients, as shown in Table 1.

a_1, a_2 are the pixel coordinate of CPIII markers' center in the image of camera A and camera B. Then insert a_1, a_2 in formula (8) and (9), we can get the point coordinates in the camera coordinate system. In the experiment, we measure the changing target point several times, the result of calculated and the measured values are shown in Table 2. We can see from the result that the accuracy of the calculated values are within 1mm.

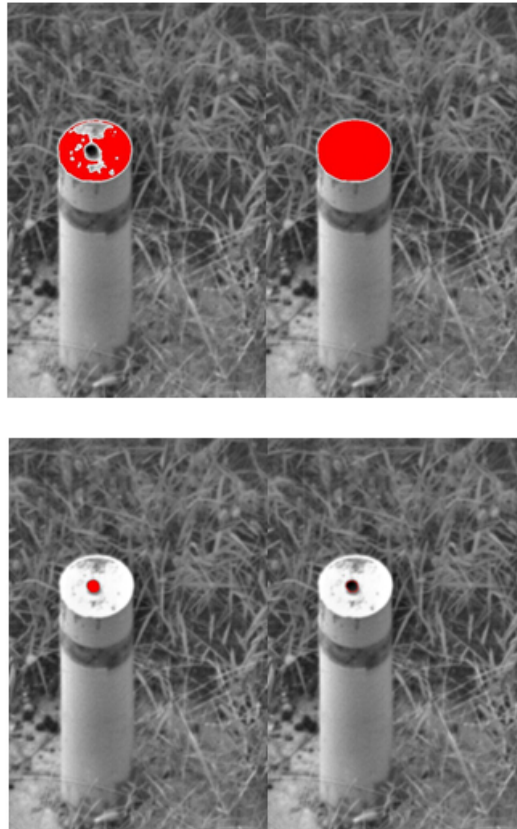


Fig. (6). The Positioning Process of Marker’s Center.

Table 1. The Parameters of Calibration.

Parameter	Value	Parameter	Value
C ₀	0.117829050067943	C ₉	0.217294442688392
C ₁	21655.6962839942	C ₁₀	4524.74939092065
C ₂	-21705.2790630025	C ₁₁	30962.047464585
C ₃	-354.547573901947	C ₁₂	871.609537957446
C ₄	2.0846111223893E-6	C ₁₃	2.59928980730993E-5
C ₅	0.396953567416608	C ₁₄	36.947336068678
C ₆	0.397929886963554	C ₁₅	-37.4694553327879
C ₇	36.981335182326	C ₁₆	3879.43487435403
C ₈	-54468.954284934	C ₁₇	771.226990483799

Table 2. The Result of Calculated and the Measured Values.

a ₁	a ₂	Calculated value x (mm)	Calculated value y (mm)	Measured Value x ₀ (mm)	Measured Value y ₀ (mm)	x ₀ -x (mm)	y ₀ -y (mm)
3072	31	1800.056111	247.1967494	1800	248	-0.056111	0.8032506
3228	187	1800.712254	297.6561236	1800	298	-0.712254	0.3438764

Table 2. contd...

a_1	a_2	Calculated value x (mm)	Calculated value y (mm)	Measured Value x_0 (mm)	Measured Value y_0 (mm)	x_0-x (mm)	y_0-y (mm)
3383	340	1800.209807	347.5076708	1800	348	-0.209807	0.4923292
3539	495	1800.321605	397.7517483	1800	398	-0.321605	0.2482517
3022	143	1900.568849	247.5016913	1900	248	-0.568849	0.4983087
3168	288	1900.598783	297.3426287	1900	298	-0.598783	0.6573713
3316	433	1899.335846	347.5362720	1900	348	0.664154	0.4637280
3610	726	1900.124767	447.7802425	1900	448	-0.124767	0.2197575
2841	106	1999.516582	198.5422300	2000	198	0.483418	-0.5422300
2976	241	2000.217096	247.2624321	2000	248	-0.217096	0.7375679
3117	380	1999.490981	297.8797145	2000	298	0.509020	0.1202855
3257	519	1999.494894	348.2072981	2000	348	0.505106	-0.2072981
2673	69	2099.257015	147.8857481	2100	148	0.742985	0.1142519
2804	200	2100.014983	197.6214694	2100	198	-0.014983	0.3785306
2936	332	2100.776072	247.7393153	2100	248	-0.776071	0.2606847
3070	463	2099.119048	298.1978073	2100	298	0.880952	-0.1978073
2522	39	2200.997408	97.8627440	2200	98	-0.997408	0.1372560
2648	163	2200.036083	147.9393541	2200	148	-0.036083	0.0606459
2773	288	2200.839533	197.7514067	2200	198	-0.839533	0.2485933
2899	413	2200.748649	247.8418503	2200	248	-0.748649	0.1581497
2505	129	2300.681041	97.8736540	2300	98	-0.681041	0.1263460
2626	249	2300.576775	148.2900274	2300	148	-0.576775	-0.2900274
2745	366	2299.466276	197.7283721	2300	198	0.533724	0.2716279
2866	486	2299.329586	248.0542093	2300	248	0.670414	-0.0542093
2376	98	2399.615076	48.4426985	2400	48	0.384924	-0.4426985
2491	213	2400.546326	98.5757570	2400	98	-0.546326	-0.5757570
2605	326	2400.382520	148.1944203	2400	148	-0.382520	-0.1944203
2719	439	2400.197291	197.7804528	2400	198	-0.197291	0.2195472
2366	178	2499.485931	48.3035745	2500	48	0.514069	-0.3035745
2476	288	2500.461314	98.3097423	2500	98	-0.461314	-0.3097423
2587	397	2499.101042	148.5938924	2500	148	0.898958	-0.5938924
2916	724	2499.459632	297.8161290	2500	298	0.540368	0.1838710
2357	252	2599.503890	48.2730962	2600	48	0.496110	-0.2730962
2462	356	2599.260544	97.8940619	2600	98	0.739456	0.1059381
2568	462	2600.251157	148.0578437	2600	148	-0.251157	-0.0578437

6. CONCLUSION

In this paper, we design a high-speed rail CPⅢ automatic detection system with multi-sensor fusion based on binocular stereo measurement technology. The system can realize automatic measurement of CPⅢ which is along the high-speed rail, it also can greatly shorten the cycle of CPⅢ control network measurement and reduce the burden of manual measurements. Through the experiments, we verify the feasibility and accuracy of the system. Tests show that the system can make good use in orbit testing field, the measurement accuracy can reach 1mm. The CPⅢ automatic detection system can also be combined with the IMU, GPS and gauge sensors and other detection tools into a small track inspection car and real time measure the orbital parameters. This will meet the CPⅢ control network retest demand and improve the CPⅢ control network retest precision. It has a simple structure and easy to detect the rail without the catenary. These are the advantages when compared with high-speed train

CONFLICT OF INTEREST

The authors confirm that this article content has no conflicts of interest.

ACKNOWLEDGEMENTS

This work is supported by Natural Science Foundation Research Project of Shaanxi, China (NO.20110476), the Basic Research program of Central Universities, China (NO.chd2011TD006), the Basic Research program of Central Universities, China (NO.chd2010JC021).

REFERENCES

- [1] W. Al-Nuaimy, A. Eriksen, and J. Gasgoyne, "Train-Mounted GPR for High-speed Rail Trackbed Inspection", In: *10th International Conference on Ground Penetrating Radal*, Deljt, Netherlands, 2004, pp. 21 -24.
- [2] S. Ono, A. Numakura, and T. Odaka, "High-speed Track Inspection Technologies", JR EAST Technical Review, pp. 9–13, 2003.
- [3] J. Santos, M. Hempel, and H. Sharif, "Sensing Techniques and Detection Methods for Train Approach Detection", In: *Proceedings of Vehicular Technology Conference (VTC Fall), IEEE 78th Las Vegas*, 2013, pp. 1-5.
- [4] H. Tsunashima, Y. Naganuma, A. Matsumoto, T. Mizuma, and H. Mori, "Japanese railway condition monitoring of tracks using in-service vehicle", In: *5th IET Conference on Railway Condition Monitoring and Non-Destructive Testing*, 2011, p. 6.
- [5] H. Tsunashima, Y. Naganuma, A. Matsumoto, T. Mizuma, and H. Mori, "Japanese railway condition monitoring of tracks using in-service vehicle", In: *5th IET Conference on Railway Condition Monitoring and Non-Destructive Testing (RCM 2011)*, 2011, pp. 1-6.
- [6] ImageMap Inc. <http://www.imagemap.com/laserrail.htm> (laserrail unattended geometry measurement system (UGMS) for service trains), 2006.
- [7] P.F. Weston, C.S. Ling, C.J. Goodman, C. Roberts, P. Li, and R.M. Goodall, "Monitoring lateral track irregularity from in-service railway vehicles", *Rail and Rapid Transit*, vol. 221, pp. 89-100 Jan 2007.
- [8] Q. Wang, S. Kang, L. Zuo, and Y. Zhou, "A novel electro-optical servo control technology and its application", In: *Fourth International Conference on Genetic and Evolutionary Computing (ICGEC)*, 2010, pp. 791-794.
- [9] B. Feng, X. Zhang, and H. Zhao, "The research of motion capture technology based on inertial measurement dependable", In: *IEEE 11th International Conference on Autonomic and Secure Computing*, 2013, pp. 238-243.
- [10] S. Zheng, X. Chai, X. An, and L. Li, "Railway track gauge inspection method based on computer vision", In: *IEEE International Conference on Mechatronics and Automation*, 2012, pp. 1292-1296.
- [11] M. Moretti, M. Triglia, and G. Maffei, "ARCHIMEDE The First European Diagnostic Train for Global Monitoring of Railway Infrastructure", In: *2004 IEEE Intelligent Vehicles Symposium, Parma, Italy*, 2004, pp. 14-17.
- [12] X. Zhang, Y. Li, J. Wang, and Y. Chen, "Design of high-speed image processing system based on FPGA", In *9th International Conference on Electronic Measurement and Instruments, ICEMI '09.*, 2010, pp. 65-69.
- [13] Y. Li, W. Wang, and S. Wei, "Data transmission system design of digital sensor in track inspection system based on CAN bus," *China Railway Science*, vol. 33, pp. 122-126, Aug. 2012.
- [14] R. Huber-Mork, M. Nolle, A. Oberhauser, and E. Fischmeister, "Statistical Rail Surface Classification Based on 2D and 21/2D Image Analysis", *Advanced Concepts For Intelligent Vision Systems Lecture note in computer*, vol. 6474, pp. 50-61, Dec. 2010.
- [15] Y. Yakimovsky, and R. Cunningham, "A system for extracting three dimensional measurement from a stereo pair of cameras". *Computer Graphics and Image Processing*, vol. 8, no. 7, pp. 195-210, 1978.
- [16] Z.Y. Zhang, "A flexible new technique for camera calibration", *IEEE Transactions on Pattern Analysis and Machine Intelligence*, vol. 11, no. 22, pp. 1330-1334, 2000.
- [17] S. Kim, and S. Chol, "The Coil recognition system for an unmanned crane using stereo vision", In: *The 30th Annual Conference of the IEEE industrial Electronic Society*, November, Busan, Korea, pp. 1235-1239, 2004.
- [18] M. Sonka, V. Hlavac, and R. Boyle. "Image Processing", *Analysis and Machine Vision (2nd Editton)*, New York: Thomson Press, 2002, pp. 460-469.

Received: September 22, 2014

Revised: November 03, 2014

Accepted: November 06, 2014

© Han et al.; Licensee Bentham Open.

This is an open access article licensed under the terms of the Creative Commons Attribution Non-Commercial License (<http://creativecommons.org/licenses/by-nc/3.0/>) which permits unrestricted, non-commercial use, distribution and reproduction in any medium, provided the work is properly cited.